Lawrence Berkeley National Laboratory
LBL Publications

Title

How Do Climate Model Resolution and Atmospheric Moisture Affect the Simulation of Unprecedented Extreme Events Like the 2021 Western North American Heat Wave?

Permalink

https://escholarship.org/uc/item/1k99s5dh

Journal

ISSN

Authors

Liu, Xue
Saravanan, Ramalingam
Fu, Dan
et al.

Publication Date

2024-07-28

DOI

Copyright Information

Peer reviewed

How Do Climate Model Resolution and Atmospheric Moisture Affect the Simulation of Unprecedented Extreme Events Like the 2021 Western North American Heat Wave?

Xue Liu[1] , Ramalingam Saravanan[2], Dan Fu[1] , Ping Chang[1,2] , Christina M. Patricola[3,4] , and Travis A. O'Brien[4,5]

[1]Department of Oceanography, Texas A&M University, College Station, TX, USA, [2]Department of Atmospheric Sciences, Texas A&M University, College Station, TX, USA, [3]Department of Geological and Atmospheric Sciences, Iowa State University of Science and Technology, Ames, IA, USA, [4]Lawrence Berkeley National Laboratory, Berkeley, CA, USA, [5]Department of Earth and Atmospheric Sciences, Indiana University, Bloomington, IN, USA

Abstract Although the 2021 Western North America (WNA) heat wave was predicted by weather forecast models, questions remain about whether such strong events can be simulated by global climate models (GCMs) at different model resolutions. Here, we analyze sets of GCM simulations including historical and future periods to check for the occurrence of similar events. High- and low-resolution simulations both encounter challenges in reproducing events as extreme as the observed one, particularly under the present climate. Relatively stronger amplitudes are observed during the future periods. Furthermore, high- and low-resolution short initialized GCM simulations are both able to reasonably predict such strong events and their associated high-pressure ridge over the WNA with a 1 week forecast lead time. Moisture sensitivity experiments further indicate a drier atmospheric moisture condition results in substantially higher near-surface temperatures in the simulated heat events.

Plain Language Summary During June 2021, an extraordinarily strong heat wave occurred over parts of Western North America (WNA). It obliterated the high temperature record there and caused severe societal and ecological impacts, and is believed to be exacerbated by climate change. Low-resolution Global Climate Models (GCMs) are currently used to quantify the atmospheric responses to climate change, even though they exhibit significant biases in their simulated climate. Their ability to predict extraordinarily strong heat wave events remains unassessed. In this study, low- and high-resolution GCM simulations are shown to be able to reproduce extraordinarily strong heat wave events in the near future, but face challenges in reproducing the events as extreme as the observed one. This highlights the role of climate change in such events. A suite of short GCM simulations initialized from observations is used to show that even low-resolution GCMs can forecast observed extreme strong heat wave events and their high-pressure ridge over WNA at short lead times. We further show that in these short-term forecasts, drier atmospheric moisture initial condition can lead to significantly higher near-surface temperature.

1. Introduction

Heat waves can cause profound damages to human well-being, agriculture, infrastructure, and the environment, as well as generate high energy demand and economic loss (Campbell et al., 2018; Robine et al., 2008; Smoyer-Tomic et al., 2003; Weinberger et al., 2020; Zuo et al., 2015). During late-June 2021, a heat wave of unprecedented magnitude occurred over Western North America (WNA) (Bratu et al., 2022; Lin et al., 2022; Mo et al., 2022; Philip et al., 2021; Thompson et al., 2022), affecting multiple highly populated cities including Seattle, Portland, and Vancouver, and resulting in numerous fatalities (Benfield, 2021; Lin et al., 2022; WMO, 2021). This June 2021 event is exceptional because it occurred a full month earlier than the climatologically warmest time and obliterated the historical temperature record for the region. The maximum temperature was far above 40°C, exceeding the previous maximum record by about 5°C (Philip et al., 2021).

Factors affecting extreme heat waves in the WNA region include the large-scale atmospheric high-pressure ridge, regional topography, and human-caused climate change (Baldwin et al., 2019; Van Oldenborgh et al., 2021; Vautard et al., 2020; Wehrli et al., 2019). During the 2021 WNA heat event, a strong large-scale high-pressure ridge appeared in the atmosphere but was not as exceptional as the temperature anomalies (Philip et al., 2021). During such events air is heated over the terrain, and the easterly winds prevent cool marine air over the Pacific

from reaching inland areas. The elevation difference between the west and east sides of the mountain ranges in WNA regions causes more diabatic heating than cooling, adding additional heating to this event. Furthermore, anomalously dry soil conditions, caused by low precipitation rates, can also contribute to the extremely high temperature due to reduced latent cooling from low evaporation rates. Studies also emphasize that such extraordinarily strong heat events are made much more likely with climate change (Fischer et al., 2021; Philip et al., 2021). A more recent study (Mo et al., 2022) illustrates that this heat wave event is closely related to a landfalling atmospheric river (AR) which transports warm and moist air into the high-pressure ridge system.

The June 2021 heat wave was predicted well in the short-term weather forecasts made by HR global weather models. But global climate models (GCMs) used for attribution studies and adaptation planning use a coarser horizontal grid due to the high computational cost of long climate simulations. Much work (Hagos et al., 2015; Kopparla et al., 2013; Roberts et al., 2020; Wick et al., 2013) has been done to assess whether weather extremes, such as extreme rainfall, tropical cyclones, and ARs, are adequately represented in coarse-resolution GCMs. Since coarse-resolution GCMs fail to resolve small-scale structures and mesoscale processes, the simulations of these weather extremes can be sensitive to model resolution. This raises the question of whether such extraordinarily strong heat waves can be adequately simulated by GCMs, which suffer from biases in their simulated climate. If we view heat wave as the surface manifestation of a large-scale high-pressure ridge in the atmosphere, we may expect that GCMs should be able to capture the essential aspects of the heat wave, although model biases could affect the details of the surface response. Indeed, Fischer et al. (2021) showed that a GCM was capable of simulating extraordinarily strong heat waves and that climate change increased the occurrence frequency of such events.

This study aims to evaluate GCMs' ability to predict extreme heat events in the WNA, similar to the one observed in 2021. By comparing HR and low-resolution GCM simulations with available observations, we attempt to address the following questions: Are such events produced in the WNA region in long climate simulations? Does model resolution matter? How do model biases in humidity affect the simulation of such heat waves? The work is focused specifically on the region (45°N–52°N, 119°W–123°W) covering the highly populated cities of Seattle, Portland, and Vancouver, which were heavily affected by the 2021 extreme heat event. The model and data descriptions are in Section 2. In Section 3, we analyze sets of GCM climate simulations at different resolutions, identify their simulated strong heat events over the WNA, and compare their amplitudes with the observed event. Then in Section 4, the question of how well such heat events can be predicted using GCMs is explored through sets of short simulations initialized from observations at forecast lead times of 3-day and 1-week. Impacts of atmospheric moisture on the prediction of extreme heat events are examined and discussed as well. A summary is presented in Section 5.

2. Observational Data and Model Descriptions

2.1. Observational Data

The observational data used here is the latest European Centre for Medium-Range Weather Forecast (ECMWF) reanalysis (ERA5) (Hersbach et al., 2020), which provides needed variables with a spatial resolution of 0.25° from January 1950 to present. The product uses a 4D variational approach to combine a vast amount of satellite and in situ observations with the ECMWF weather forecast model. ERA5 is also used to create initial condition files for initialized short simulations, which are described in detail in the model description section. Furthermore, we also use HadGHCND (Caesar et al., 2006), which provides observed daily near-surface maximum and minimum temperatures, as the reliable reference for studying global heat wave properties.

2.2. Model Descriptions

2.2.1. Climate Simulations

GCM simulations were carried out using the Community Earth System Model (CESM) version 1.3 (Meehl, Yang, et al., 2019). Model tuning was carried out as described by Chang et al. (2020). Pairs of control (CTRL) and historical and future transient (HF-TNST) simulations were carried out, with both atmosphere–only and coupled configurations, following the high-resolution model intercomparison project protocol (Haarsma et al., 2016). In CTRL, the climate forcings were set to the 1950 conditions and kept constant throughout the simulations. The HF-TNST simulations were branched from CTRL and used historical radiative forcing from 1950 to 2014 and the

high-emission Representative Concentration Pathway 8.5 (RCP8.5) scenario for the future period 2015–2100. (The use of RCP8.5 as a business-as-usual scenario has come under some criticism recently, but the different scenarios do not diverge very much in the near-term future that is of concern to this study.)

Uncoupled atmosphere-only simulations share the same settings as in coupled simulation, but the transient simulations ended in 2050. Boundary SST and sea-ice forcing were prescribed from HadISST2.2.0 (Titchner & Rayner, 2014) for the period 1950–2015. Broadly following Mizuta (2008), 2016–2050 future SST and sea-ice were reconstructed by combining the CMIP5 multi-model ensemble mean projected trend with the detrended 1980–2014 observation. We refer to Haarsma et al. (2016) for more technical details. The experiments comprise two different horizontal resolutions, using consistent forcing data sets. All HR runs have a nominal horizontal resolution of 0.25° for the atmosphere and land models, and nominal 0.1° for the ocean and sea-ice models. And for the low resolution (LR) runs, the horizontal resolution is nominally 1° for all component sets.

The CESM version 2 large-ensemble (CESM2-LE), with nominal horizontal resolution of 1°, was used to examine the role of internal climate fluctuations. The coupled model configuration is described in Rodgers et al. (2021). The simulations cover the period 1850–2100, following the historical and SSP3-7.0 forcing protocols provide by CMIP6 (Eyring et al., 2016). One hundred ensemble members are available, initialized from various years of a preindustrial simulation conducted with CESM2 (Danabasoglu et al., 2020). In this study, we used only the first 50 members which follow CMIP6 protocols with biomass burning (Danabasoglu et al., 2020). Another set of 50 members using the smoothed biomass burning fluxes was not included in this analysis.

2.2.2. Short Initialized Forecast Simulations

To test the GCM's ability to forecast extraordinarily strong heat wave events, short forecast ensembles initialized from ERA5 were conducted using the Energy Exascale Earth System Model (E3SM) atmosphere model version 1 (EAM,v1) at both low- (nominal 1°) and high- (0.25°) resolutions (Leung et al., 2020). Each EAM ensemble includes 20 members with the random temperature perturbations on the order of 10^{-2}K. Given that the WNA heat event started on 27 June 2021, we initialized the forecast ensembles on June 20 and June 24, to examine the models' predictability at forecast lead times of 1 week and 3 days, respectively. The initial conditions are generated using the InitaLIzed-ensemble Analysis/Development (ILIAD; O'Brien et al., 2016) framework, with input from the ERA5 reanalysis. The forcing sea surface temperature and sea ice concentration are derived from 1-degree HadISST1 (Rayner et al., 2003) daily outputs for both LR and HR. Each forecast ensemble continues until 6 July 2021, ensuring a thorough coverage of the 2021 WNA heat event.

2.2.3. Moisture-Sensitivity Simulations

E3SM sensitivity forecasts with reduced or enhanced moisture supply at low-resolution (1°) were configured to test the response of extreme heat events to atmospheric moisture biases. Six experiments, comprised of three with reduced-moisture and three with enhanced-moisture configurations, were conducted and compared with the original LR initialized simulations. Other configuration settings were the same as in the original LR initialized runs, except that either the initial condition of specific humidity at all vertical levels (Q−/Q+), or the model's evaporation exchange coefficient (E−/E+), or both (Q − E−/Q + E+) were reduced/enhanced by 20%. The choice of 20% amplitude for the moisture perturbation was motivated by the magnitude of the climatological moisture bias in the E3SM control simulations, which is of the order of ∼20% (Figure S1 in Supporting Information S1). Therefore, the sensitivity forecasts provide an assessment of the potential impact of climate model moisture biases on the simulation of extreme heat waves.

3. Extreme Heat Events in Climate Simulations

3.1. Heat Events With Extraordinarily High Temperature

Before analyzing extreme heat events, we first compare the 2 m temperature (T2m) bias in LR and HR HF-TNST for both the coupled and uncoupled configurations (Figure S2 in Supporting Information S1). Uncoupled simulations in both LR and HR exhibit small T2m biases across the target region, with area-averaged values of ∼0.62°C in LR and ∼0.83°C in HR. Although increasing the coupled model resolution can significantly reduce the surface temperature bias over the ocean (Chang et al., 2020), T2m bias over our target land area is much more pronounced in HR than in LR coupled simulation. The area-averaged bias is ∼−0.66°C in LR coupled simulation,
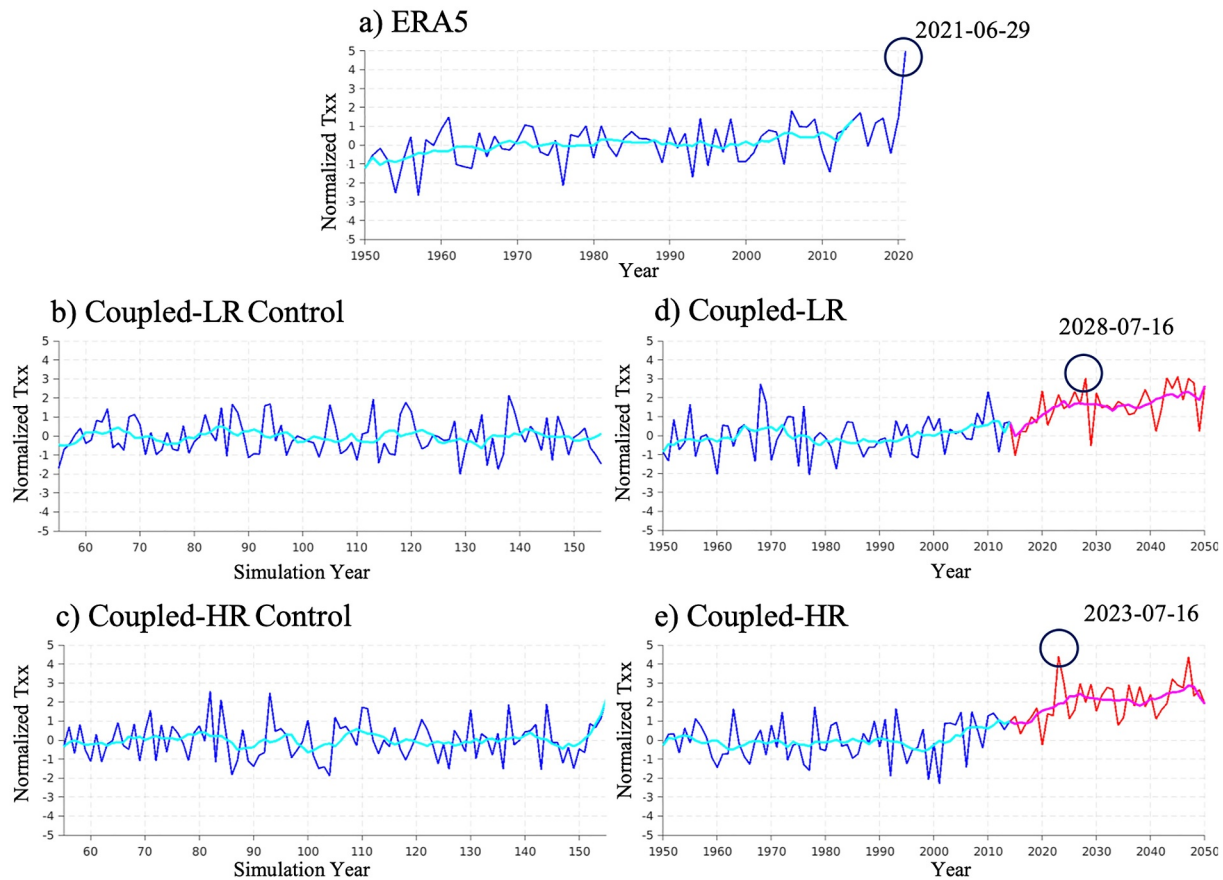
Figure 1. Area (45°N–52°N, 119°W–123°W) averaged TXx (annual maximum of daily maximum temperature) as a function of time in panels (a) observation, (b) low resolution (LR) & (c) high-resolution (HR) coupled CTRL, and (d) LR & (e) HR HF-TNST simulations over historical (blue: historical timeseries; cyan:10-year running mean of historical values) and future (RCP8.5) period (red: future timeseries; magenta: 10-year running mean of future values). The values are normalized by the historical standard deviation. Circles indicates the selected examples of exceptional extreme events whose amplitudes are larger than 3σ.

but is ~2.79°C in HR coupled simulation over WNA region. A preliminary comparison of surface soil moisture between the coupled HR simulation and ERA5 indicates this HR coupled simulation significantly underestimates the soil moisture (Figure S3 in Supporting Information S1), contributing to the high T2m bias in HR coupled simulation. Further analysis of the land model in this HR coupled simulation is planned, but is beyond the scope of this study.

Next, we compare the extreme heat events between model simulations and observations, defining a heat event based on the annual maximum of daily maximum temperature, TXx. To exclude the direct impact of mean temperature bias on the amplitude of extreme heat events, we normalize their temperature based on each model's own historical mean and standard deviations. Figure 1 show the TXx timeseries averaged over the WNA region and their 10-year running mean in CESM coupled climate simulations compared to that derived from ERA5. Observed temperatures exhibit a trend of about 3.7°C increase over the period from 1950 to 2014 in this region (not shown). During the 2021 WNA heat event, the observed TXx anomaly was exceptional—its value of 5°C was higher than the previous maximum record, with the anomaly exceeding 5 times the historical standard deviation (σ: ~1.64°C) (Figure 1a). However, the HF-TNST simulations fail to replicate the 5σ amplitude of the extreme event. Under the 1950 climate forcing, CTRL does not show an increasing trend and simulates weaker heat events, with most of their amplitudes falling within 2σ at both HR and LR (Figures 1b and 1c). In contrast, HF-TNST can reproduce cases of heat events with relatively intense amplitudes (Figures 1d and 1e). During the future period, under the RCP8.5 forcing, both LR and HR HF-TNST simulate heat events with amplitudes exceeding 3 times their own historical standard deviation (σ (LR: 1.79°C; HR: 1.71°C). Note that the dry soil bias in HR coupled HF-TNST tends to enhance the amplitude of the heat events. However, even with this dry bias, HR

coupled HF-TNST still falls short in simulating the strong amplitudes of the heat waves. Uncoupled LR and HR simulations show results consistent with coupled simulations.

We further extend our investigation using CESM2-LE to increase our sample size and confirm the robustness of our results in the presence of internal variability. The low-resolution CESM2-LE simulations (Figure S4 in Supporting Information S1) show that climate change increases the number of intense heat events, affirming its role in amplifying the risk of extraordinarily strong heat events. Before 2050, most ensemble members fail to capture the 5σ extreme heat event over the WNA region. Only after 2050, a considerable number of ensemble members demonstrate the ability to simulate extreme heat events with temperature anomalies higher than 5σ with respect to the historical climate mean (Figure S4 in Supporting Information S1). These findings generally suggest that both LR and HR GCMs' climate simulations can produce outstanding heat events, but fall short in capturing the observed extremity in amplitude, as seen in the 2021 WNA heat wave, particularly under present climate conditions. The results underscore the importance of climate change in influencing extreme heat events. Based on the current evidence, increasing model resolution does not appear to lead to significant improvements in this case.

### 3.2. Observed Versus Simulated High-Pressure Ridge System

The evolution of the extreme heat wave is controlled by the large-scale atmospheric circulation. The observed and simulated high-pressure systems linked to the extreme heat events are compared in Figure 2 (left) to validate the GCM's ability reproduce the dominant circulation patterns that drive the heat wave. The annual maximum geopotential height at 500 hPa (Z500) (Figure 2 left) displays a high-pressure ridge system occurring during the extreme heat events. Both LR and HR are able to reproduce such spatial patterns of high-pressure ridge with the peaks of the ridge leading the temperature peaks (Figure 2 right).

The timeseries of annual maximum Z500 over the WNA region in the observation and in the simulations are shown in Figure S5 in Supporting Information S1. Long-term increasing trends of Z500 caused by thermal expansion (Christidis & Stott, 2015) are observed in both the observation and the HF-TNST. However, observed and simulated extremes exhibit some differences. In observations, compared with the 5σ anomalous TXx, the Z500 anomaly is only exceeds 3σ, suggesting there must be other factors, such as moist processes, causing nonlinear amplification of this extraordinary event near the surface.

Previous studies have noted that low soil moisture leads to higher temperatures during heat waves through nonlinear effects (Hauser et al., 2016; Mueller & Seneviratne, 2012; Seneviratne et al., 2010). A recent investigation by Bartusek et al. (2022) reveals that the physical drivers of the record-breaking 2021 WNA heat event stem from the associated atmospheric circulation and land-atmosphere feedbacks. The regional temperature continued to rise during this heat event after the geopotential height had peaked, which is attributable to the presence of dry soil moisture anomalies. From March until the occurrence of this event, over the region from southern British Columbia to California, precipitation was anomalously weak, causing the antecedent dry condition which contributed to the exceptionally high temperature anomalies (Philip et al., 2021). This land-atmosphere feedbacks likely amplified the severity of the event by about 40% (Bartusek et al., 2022). Another recent study (Mo et al., 2022) suggests that a landfalling AR occurring before and during the heat event, transported warm and moist air into the high-pressure ridge system, also contributing to the exceptionally high temperatures. In addition, limited studies (Liu et al., 2020; Pranindita et al., 2022) have also suggested that reduced air moisture, leading to reduced precipitation, contributes to the long duration of heat waves, such as the ones occurred in Europe in 2003 and 2010. All these processes may contribute to the fact that the temperature anomalies are more exceptional than the local Z500 anomaly in the observed heat event. However, in the HF-TNST GCM simulations, temperature anomalies during typical extraordinary heat wave events have similar normalized magnitudes to the atmospheric circulation patterns anomalies (both are ~3σ), unlike what is seen in the observations. These findings are consistent for both coupled and uncoupled climate simulations (Figure S6 in Supporting Information S1). This observed discrepancy between simulations and observations motivates us to explore in the next section why temperature anomalies simulated in model are not as exceptional as in the observations.

## 4. Predictability of 2021 WNA Heat Event Using GCMs

Short simulations initialized from reanalyzed observations allow us to examine the questions of whether such an extraordinary heat event can be forecast by GCMs and whether grid resolution makes a difference. Previous
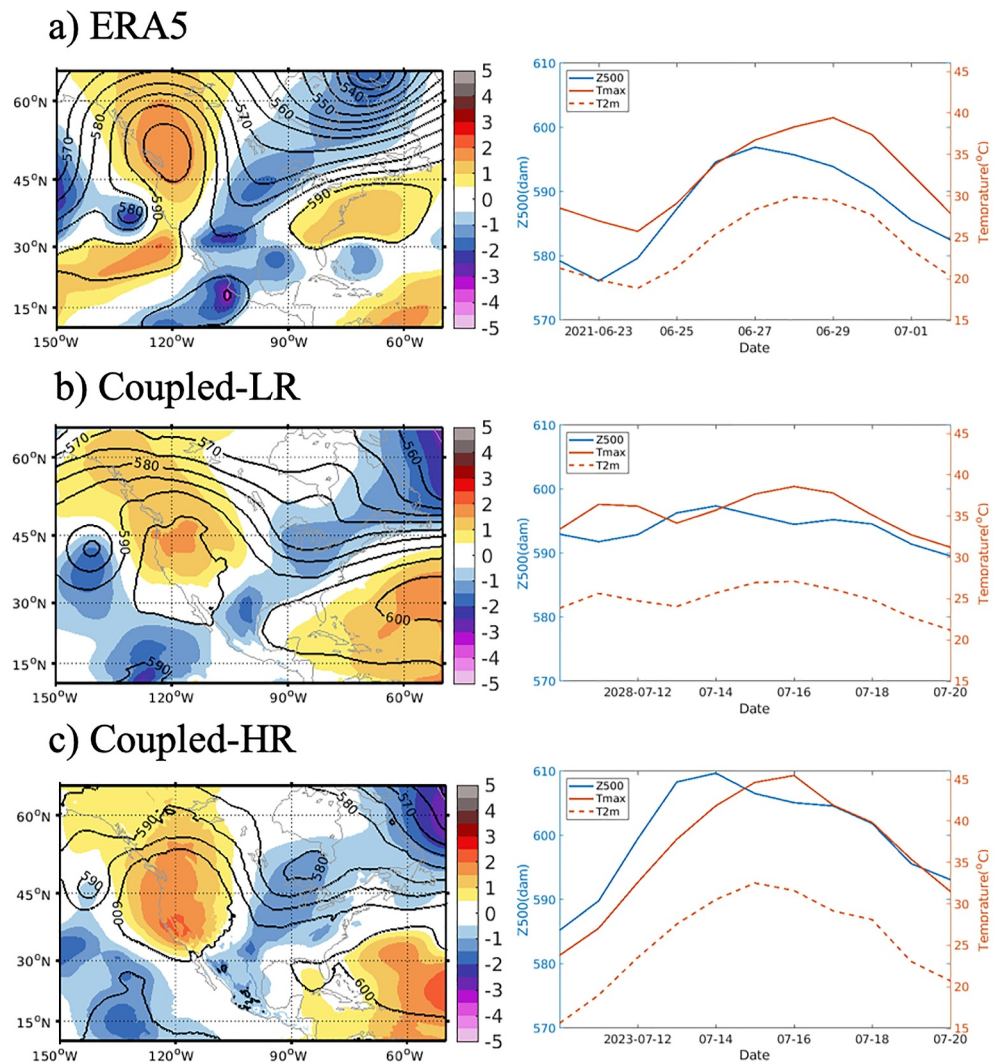
Figure 2. Left: annual maximum geopotential height at 500 hPa (Z500) (contours: unit: dam) and its normalized values (color) over Western North America region when selected extreme heat events occur in panels (a) ERA5; (b) Coupled-LR and (c) Coupled-HR. Right: Area (45°N–52°N, 119°W–123°W) averaged daily temperature (blue) and maximum temperature (red) when selected extreme heat events occur in (a) ERA5; (b) Coupled-LR and (c) Coupled-HR. Corresponding heat events are circled in Figure 1.

studies (Emerton et al., 2022; Lin et al., 2022; White et al., 2023) have highlighted the capabilities of weather forecast systems in predicting the 2021 WNA heat wave event. While forecasts 5 days before the event's peak showed good accuracy in predicting its onset and duration, forecasted high-temperature records in many ensembles still fell 1–3°C short of the observed high (White et al., 2023). Sub-seasonal forecasts indicate an increased probability of extreme heat with lead times of 10–20 days (Lin et al., 2022; White et al., 2023).

Figure 3 shows the predicted TXx and high-pressure ridge system over WNA during the 2021 heat wave at a forecast lead time of 3 days using LR and HR GCM. As the GCM employed here lacks integration with a data assimilation system, we initialized forecasts using ERA5 reanalysis instead of a data assimilation product consistent with the GCM. This introduces an "initialization shock" that impacts the model's ability to accurately reproduce the observed event. While incorporating a data assimilation system into the GCM can address the mismatch with observations and increase the prediction accuracy, it is beyond the scope of this study. Despite this limitation, our model performance appears reasonable when compared to the disparities in simulated extreme heat summers between ERA5 and CMIP6 simulations (Dong et al., 2023), as well as the shortcomings identified in other weather forecast ensembles (Lin et al., 2022; White et al., 2023). Both LR and HR can reasonably predict the
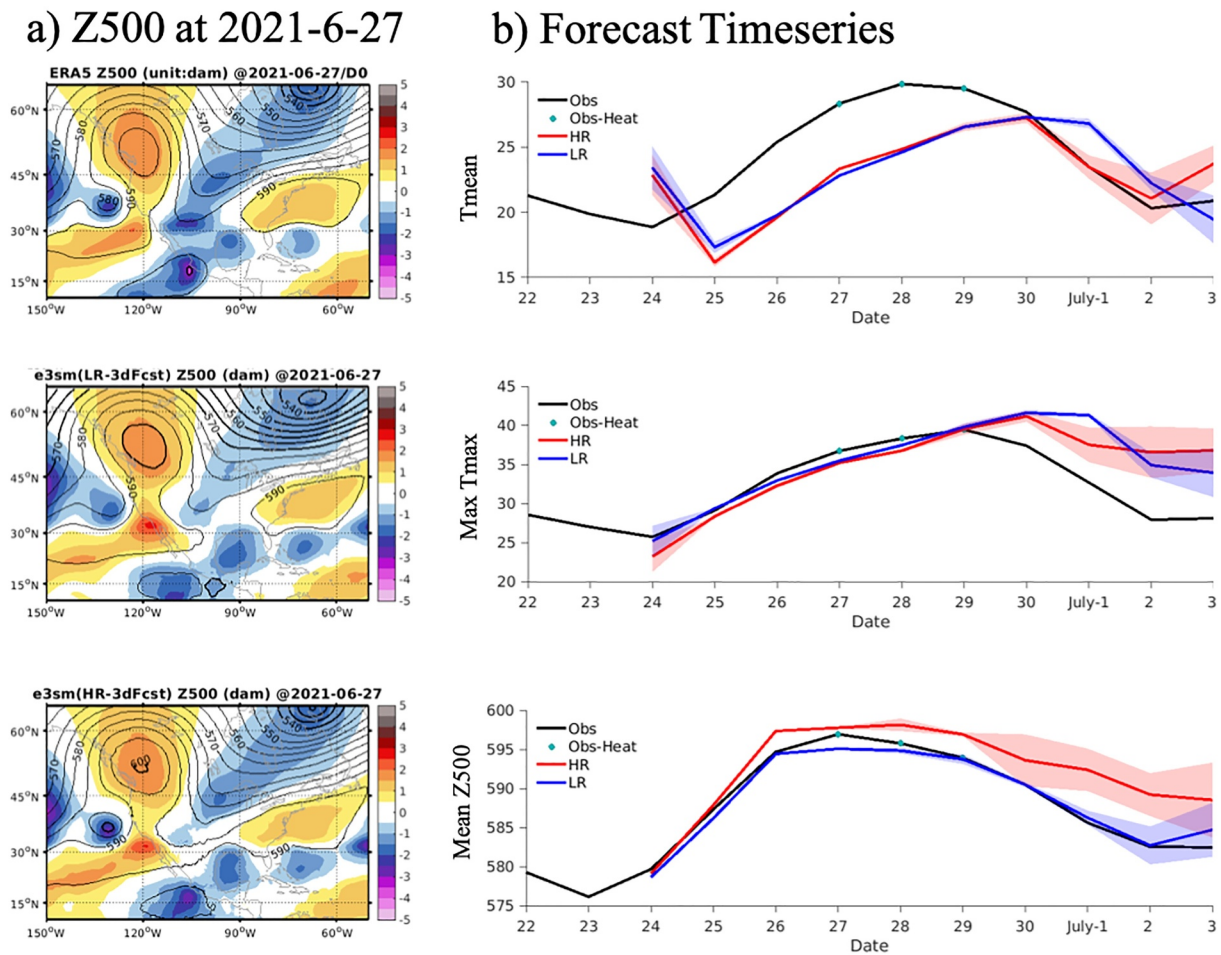
Figure 3. (a) observed (top) and predicted (middle: low resolution (LR) and bottom: HR) annual maximum geopotential height at 500 hPa (Z500) (contour; unit: dam) and their normalized values (color) over Western North America (WNA) region at 2021/06/27 when 2021 WNA heat event occurred. The prediction is at forecast lead time of 3 days. (b) Timeseries of observed and simulated area (45°N–52°N, 119°W–123°W) averaged daily mean temperature (top: Tmean; unit: °C), maximum temperature (middle: Max Tmax; unit: °C) and Z500 (bottom; unit: dam). Black solid lines are from ERA5, Blue thick lines are from LR 3-day forecast run, red thick lines are from high-resolution 3-day forecast run. Shading indicates the ensemble spread when using initial perturbations on the order of $1e^{-2}$.

observed anomalous high TXx as well as the high-pressure ridge system over WNA during 2021 heat wave at forecast lead times of 3 days. The forecast results remain similar at a forecast lead time of 1 week. This confirms, once again, that even a coarse-resolution GCM is capable of capturing extreme heat wave events.

GCMs always exhibit some biases in the flow and moisture fields in reproducing the observed mean climate (Figure S1 in Supporting Information S1). As noted above, dry conditions likely contributed to the exceptional high temperature during the 2021 WNA heat event (Liu et al., 2020; Mo et al., 2022; Pranindita et al., 2022). We carried out further GCM forecasts to investigate the impact of atmospheric moisture content on the magnitude and timing of the heat wave. In these forecast experiments, we changed the evaporation or initial moisture input, or both, to test the sensitivity of heat waves to atmospheric moisture content.

Our results show that changing the evaporation coefficient does not affect the strength of heat waves (Figure S7 in Supporting Information S1) whereas changing the initial condition of atmospheric moisture does (Figure 4). When the ground is already dry, changing the evaporation coefficient will not exert a large influence on the atmospheric moisture. At short timescales, the atmospheric moisture content has limited sensitivity to the evaporation coefficient change, and instead is more strongly influenced by the memory of the initial condition. Forecasts with the drier initial conditions have a significant impact on the simulated heat wave. For a 1-week forecast lead time, decreasing initial moisture input by 20% can amplify the maximum daily temperature of this event by about 2°C and extend duration with high TXx by 2 days, as well as extending the persistence of the
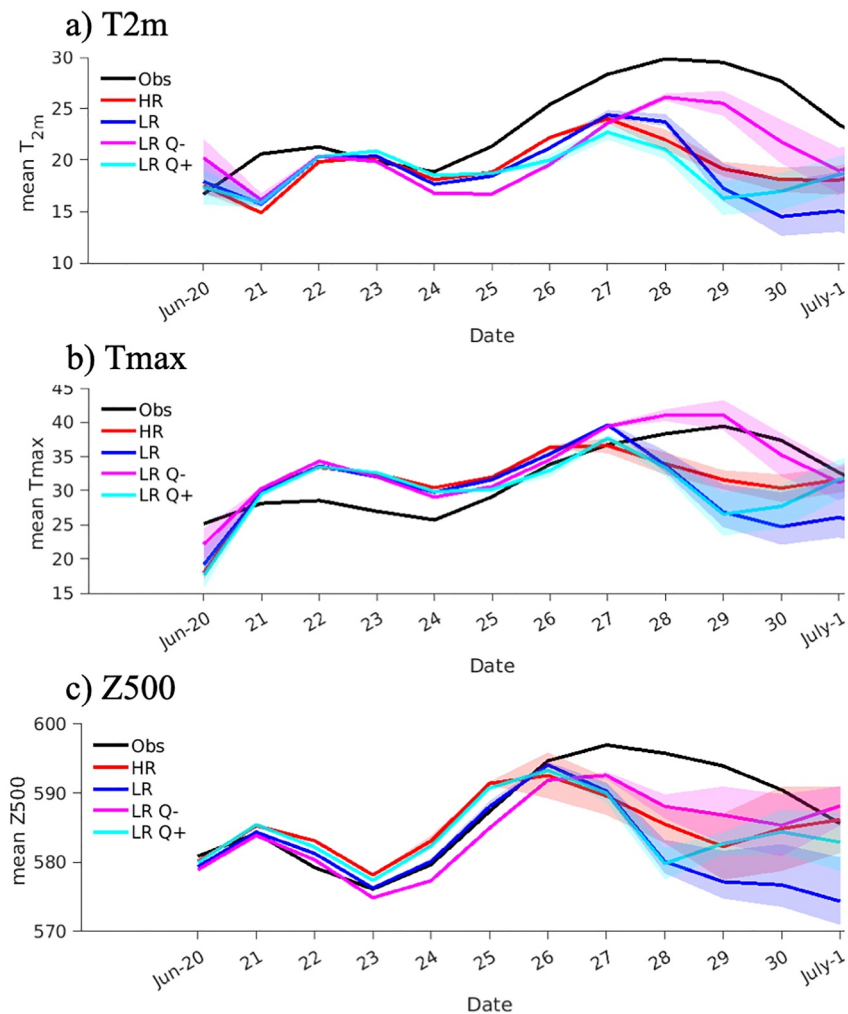
Figure 4. Timeseries of observed and simulated area (45°N–52°N, 119°W–123°W) averaged daily temperature (top; unit: °C), maximum temperature (middle; unit: °C), and Z500 (bottom; unit: dam) from ERA5 (Black lines), low resolution 1 week forecast run (Blue lines), high-resolution 1 week forecast run (Red Lines), moisture-reduced (Magenta) and moisture-enhanced (Cyan) experiments. Here, the moisture-changed experiments are designed through modifying the initial moisture input (Q+/−). Shading indicates the ensemble spread when using initial perturbations on the order of $1e^{-2}$.

large-scale high-pressure system for 1 more day. Higher moisture typically contributes to increased clouds and enhanced rainfall, subsequently reducing near-surface temperature (Liu et al., 2020; Pranindita et al., 2022; White et al., 2023). Conversely, drier unsaturated air conditions lead to more prolonged clear skies, posing challenges for temperature reduction. The finding is consistent with the previous studies that demonstrate the impact of drier air conditions as a contributing factor to the long duration of past high-impact European and Russian heat waves (Liu et al., 2020; Pranindita et al., 2022). Specifically, we observe an approximately 2°C increase in the simulated heat wave due to drier air conditions.

Although the strength of large-scale high-pressure ridge had no significant change for drier initial conditions, the longer persistence caused by the dryness can contribute to the enhancement of the strong heat wave. As mentioned above, model resolution does not seem to matter much, as compared to moisture content, in determining the strength of heat wave. Given that GCMs can exhibit significant moisture bias, the fidelity of their simulated heat events may benefit more from reduction in the moisture bias rather than an increase in model resolution, though simulation of other extreme events, like intense precipitation, could benefit significantly from increased model resolution. Other factors, such as soil moisture and anthropogenic global warming (Bartusek et al., 2022; Zhang et al., 2023), can also affect the simulation of heat waves, but they are not the focus of this study.

5. Conclusion

We demonstrate that both high- and low-resolution GCMs can simulate strong heat wave events (temperature anomalies: ∼3σ), but fall short in capturing the extraordinarily high temperature (temperature anomalies: ∼5σ), as seen in the 2021 WNA case, particularly under the present climate conditions. Although we have not carried out a formal attribution study, the amplification in extreme heat wave strengths between the historical and future simulations provides an indication that anthropogenic climate change makes such extreme heat waves more likely. We carried out short-term (2–7 days) forecasts using a low- and HR GCM, and found that in both cases the forecast of the heat wave was quite similar—the atmospheric flow pattern associated with this extreme heat wave was forecasted reasonably well, even at coarse-resolution. This is consistent with the notion that heat waves are driven by the large-scale atmospheric circulation patterns that are resolved by GCMs. However, the forecasted near-surface temperature anomalies were weaker compared to observations at both resolutions. A moisture-sensitivity test of the forecasts shows that a drier initial condition can extend the persistence of the heat wave and amplify the forecasted mean near-surface temperature anomalies. This suggests that reducing the moisture bias in GCMs is crucial for improving the simulation of heat waves in GCMs.

Data Availability Statement

The Community Earth System Model (CESM) (Meehl et al., 2019) developed by the National Center for Atmospheric Research (NCAR) can be downloaded online (https://escomp.github.io/CESM/versions/cesm2.1/html/downloading_cesm.html). The climate simulations used in this work are available from the following data portal (https://ihesp.github.io/archive/products/ds_archive/CESM-HRMIP.html). Detailed data descriptions are in Chang et al. (2020). And the CESM2 large-ensembles (Danabasoglu et al., 2020) are available on https://www.earthsystemgrid.org/dataset/ucar.cgd.cesm2le.output.html and on the ICCP Live Access server (LAS) https://climatedata.ibs.re.kr/las. The downloading Energy Exascale Earth System Model (E3SMv1) (Leung et al., 2020) code is available at https://dx.doi.org/10.11578/E3SM/dc.20210927.1, and its short forecast simulations are available at https://zenodo.org/badge/latestdoi/466282870 (Liu, 2022). https://doi.org/10.5281/zenodo.6336008.

References

Baldwin, J. W., Dessy, J. B., Vecchi, G. A., & Oppenheimer, M. (2019). Temporally compound heat wave events and global warming: An emerging hazard. *Earth's Future*, 7(4), 411–427. https://doi.org/10.1029/2018ef000989

Bartusek, S., Kornhuber, K., & Ting, M. (2022). 2021 North American heatwave amplified by climate change-driven nonlinear interactions. *Nature Climate Change*, 12(12), 1143–1150. https://doi.org/10.1038/s41558-022-01520-4

Benfield. (2021). A. Global catastrophe recap september 2021 (PDF) (Report) (p. 13). Retrieved from http://thoughtleadership.aon.com/Documents/20210012-analytics-if-september-global-recap.PDF

Bratu, A., Card, K. G., Closson, K., Aran, N., Marshall, C., Clayton, S., et al. (2022). The 2021 Western North American heat dome increased climate change anxiety among British Columbians: Results from a natural experiment. *The Journal of Climate Change and Health*, 6, 100116. https://doi.org/10.1016/j.joclim.2022.100116

Caesar, J., Alexander, L., & Vose, R. (2006). Large-scale changes in observed daily maximum and minimum temperatures: Creation and analysis of a new gridded data set. *Journal of Geophysical Research*, 111(D5). https://doi.org/10.1029/2005jd006280

Campbell, S., Remenyi, T. A., White, C. J., & Johnston, F. H. (2018). Heatwave and health impact research: A global review. *Health & Place*, 53, 210–218. https://doi.org/10.1016/j.healthplace.2018.08.017

Chang, P., Zhang, S., Danabasoglu, G., Yeager, S. G., Fu, H., Wang, H., et al. (2020). An unprecedented set of high-resolution earth system simulations for understanding multiscale interactions in climate variability and change [Dataset]. *Journal of Advances in Modeling Earth Systems*, 12, 12. https://doi.org/10.1029/2020MS002298

Christidis, N., & Stott, P. A. (2015). Changes in the geopotential height at 500 hPa under the influence of external climatic forcings. *Geophysical Research Letters*, 42(24), 10–798. https://doi.org/10.1002/2015gl066669

Danabasoglu, G., Lamarque, J. F., Bacmeister, J., Bailey, D. A., DuVivier, A. K., Edwards, J., et al. (2020). The community earth system model version 2 (CESM2) [Software]. *Journal of Advances in Modeling Earth Systems*, 12(2). https://doi.org/10.1029/2019MS001916

Dong, Z., Wang, L., Xu, P., Cao, J., & Yang, R. (2023). Heatwaves similar to the unprecedented one in summer 2021 over western North America are projected to become more frequent in a warmer world. *Earth's Future*, 11(2), e2022EF003437. https://doi.org/10.1029/2022ef003437

Emerton, R., Brimicombe, C., Magnusson, L., Roberts, C., Di Napoli, C., Cloke, H. L., & Pappenberger, F. (2022). Predicting the unprecedented: Forecasting the June 2021 Pacific Northwest heatwave. *Weather*, 77(8), 272–279. https://doi.org/10.1002/wea.4257

Eyring, V., Bony, S., Meehl, G. A., Senior, C. A., Stevens, B., Stouffer, R. J., & Taylor, K. E. (2016). Overview of the Coupled Model Intercomparison Project Phase 6 (CMIP6) experimental design and organization. *Geoscientific Model Development*, 9(5), 1937–1958. https://doi.org/10.5194/gmd-9-1937-2016

Fischer, E. M., Sippel, S., & Knutti, R. (2021). Increasing probability of record-shattering climate extremes. *Nature Climate Change*, 11(8), 689–695. https://doi.org/10.1038/s41558-021-01092-9

Haarsma, R. J., Roberts, M. J., Vidale, P. L., Senior, C. A., Bellucci, A., Bao, Q., et al. (2016). High resolution model intercomparison project (HighResMIP v1. 0) for CMIP6. *Geoscientific Model Development*, 9(11), 4185–4208. https://doi.org/10.5194/gmd-9-4185-2016

Hagos, S., Leung, L. R., Yang, Q., Zhao, C., & Lu, J. (2015). Resolution and dynamical core dependence of atmospheric river frequency in global model simulations. *Journal of Climate*, 28(7), 2764–2776. https://doi.org/10.1175/jcli-d-14-00567.1

Hauser, M., Orth, R., & Seneviratne, S. I. (2016). Role of soil moisture versus recent climate change for the 2010 heat wave in western Russia. *Geophysical Research Letters*, *43*(6), 2819–2826. https://doi.org/10.1002/2016gl068036

Hersbach, H., Bell, B., Berrisford, P., Hirahara, S., Horányi, A., Muñoz-Sabater, J., et al. (2020). The ERA5 global reanalysis. *Quarterly Journal of the Royal Meteorological Society*, *146*(730), 1999–2049. https://doi.org/10.1002/qj.3803

Kopparla, P., Fischer, E. M., Hannay, C., & Knutti, R. (2013). Improved simulation of extreme precipitation in a high-resolution atmosphere model. *Geophysical Research Letters*, *40*(21), 5803–5808. https://doi.org/10.1002/2013gl057866

Leung, L. R., Bader, D. C., Taylor, M. A., & McCoy, R. B. (2020). An introduction to the E3SM special collection: Goals, science drivers, development, and analysis [Software]. *Journal of Advances in Modeling Earth Systems*, *12*(11). e2019MS001821. https://doi.org/10.1029/2019MS001821

Lin, H., Mo, R., & Vitart, F. (2022). The 2021 western North American heatwave and its subseasonal predictions. *Geophysical Research Letters*, *49*(6), e2021GL097036. https://doi.org/10.1029/2021gl097036

Liu, X. (2022). xuetamu/e3sm_short_term_forecasts_2021: 2021_heatwave_e3sm_short_forecast (Forecast). [Software]. *Zenodo*. https://doi.org/10.5281/zenodo.6336008

Liu, X., He, B., Guo, L., Huang, L., & Chen, D. (2020). Similarities and differences in the mechanisms causing the European summer heatwaves in 2003, 2010, and 2018. *Earth's Future*, *8*(4), e2019EF001386. https://doi.org/10.1029/2019ef001386

Meehl, G. A., Yang, D., Arblaster, J. M., Bates, S. C., Rosenbloom, N., Neale, R., et al. (2019). Effects of model resolution, physics, and coupling on Southern Hemisphere storm tracks in CESM1.3 [Software]. *Geophysical Research Letters*, *46*(21), 12408–12416. https://doi.org/10.1029/2019GL084057

Mizuta, R. (2008). Estimation of the future distribution of sea surface temperature and sea ice using the CMIP3 multi-model ensemble mean CMIP3. *Technical Reports of the Meteorological Research Institute*, *56*, 1.

Mo, R., Lin, H., & Vitart, F. (2022). An anomalous warm-season trans-Pacific atmospheric river linked to the 2021 western North America heatwave. *Communications Earth & Environment*, *3*(1), 1–12. https://doi.org/10.1038/s43247-022-00459-w

Mueller, B., & Seneviratne, S. I. (2012). Hot days induced by precipitation deficits at the global scale. *Proceedings of the National Academy of Sciences of the United States of America*, *109*(31), 12398–12403. https://doi.org/10.1073/pnas.1204330109

O'Brien, T. A., Collins, W. D., Kashinath, K., Rübel, O., Byna, S., Gu, J., et al. (2016). Resolution dependence of precipitation statistical fidelity in hindcast simulations. *Journal of Advances in Modeling Earth Systems*, *8*(2), 976–990. https://doi.org/10.1002/2016ms000671

Philip, S. Y., Kew, S. F., & Oldenborgh, G. J. (2021). *Rapid attribution analysis of the extraordinary heatwave on the Pacific Coast of the US and Canada June 2021* (Vol. 37). World Weather Attribution.

Pranindita, A., Wang-Erlandsson, L., Fetzer, I., & Teuling, A. J. (2022). Moisture recycling and the potential role of forests as moisture source during European heatwaves. *Climate Dynamics*, *58*(1–2), 609–624. https://doi.org/10.1007/s00382-021-05921-7

Rayner, N. A. A., Parker, D. E., Horton, E. B., Folland, C. K., Alexander, L. V., Rowell, D. P., et al. (2003). Global analyses of sea surface temperature, sea ice, and night marine air temperature since the late nineteenth century. *Journal of Geophysical Research*, *108*(D14). https://doi.org/10.1029/2002jd002670

Roberts, M. J., Camp, J., Seddon, J., Vidale, P. L., Hodges, K., Vannière, B., et al. (2020). Projected future changes in tropical cyclones using the CMIP6 HighResMIP multimodel ensemble. *Geophysical Research Letters*, *47*(14), e2020GL088662. https://doi.org/10.1029/2020gl088662

Robine, J. M., Cheung, S. L. K., Le Roy, S., Van Oyen, H., Griffiths, C., Michel, J. P., & Herrmann, F. R. (2008). Death toll exceeded 70,000 in Europe during the summer of 2003. *Comptes Rendus Biologies*, *331*(2), 171–178. https://doi.org/10.1016/j.crvi.2007.12.001

Rodgers, K. B., Lee, S. S., Rosenbloom, N., Timmermann, A., Danabasoglu, G., Deser, C., et al. (2021). Ubiquity of human-induced changes in climate variability. *Earth System Dynamics*, *12*(4), 1393–1411. https://doi.org/10.5194/esd-12-1393-2021

Seneviratne, S. I., Corti, T., Davin, E. L., Hirschi, M., Jaeger, E. B., Lehner, I., et al. (2010). Investigating soil moisture–climate interactions in a changing climate: A review. *Earth-Science Reviews*, *99*(3–4), 125–161. https://doi.org/10.1016/j.earscirev.2010.02.004

Smoyer-Tomic, K. E., Kuhn, R., & Hudson, A. (2003). Heat wave hazards: An overview of heat wave impacts in Canada. *Natural Hazards*, *28*(2/3), 465–486. https://doi.org/10.1023/a:1022946528157

Thompson, V., Kennedy-Asser, A. T., Vosper, E., Lo, Y. E., Huntingford, C., Andrews, O., et al. (2022). The 2021 western North America heat wave among the most extreme events ever recorded globally. *Science Advances*, *8*(18), eabm6860. https://doi.org/10.1126/sciadv.abm6860

Titchner, H. A., & Rayner, N. A. (2014). The Met Office Hadley Centre sea ice and sea surface temperature data set, version 2: 1. Sea ice concentrations. *Journal of Geophysical Research: Atmospheres*, *119*(6), 2864–2889. https://doi.org/10.1002/2013JD020316

Van Oldenborgh, G. J., van der Wiel, K., Kew, S., Philip, S., Otto, F., Vautard, R., et al. (2021). Pathways and pitfalls in extreme event attribution. *Climatic Change*, *166*(1), 1–27. https://doi.org/10.1007/s10584-021-03071-7

Vautard, R., van Aalst, M., Boucher, O., Drouin, A., Haustein, K., Kreienkamp, F., et al. (2020). Human contribution to the record-breaking June and July 2019 heatwaves in Western Europe. *Environmental Research Letters*, *15*(9), 094077. https://doi.org/10.1088/1748-9326/aba3d4

Wehrli, K., Guillod, B. P., Hauser, M., Leclair, M., & Seneviratne, S. I. (2019). Identifying key driving processes of major recent heat waves. *Journal of Geophysical Research: Atmospheres*, *124*(22), 11746–11765. https://doi.org/10.1029/2019jd030635

Weinberger, K. R., Harris, D., Spangler, K. R., Zanobetti, A., & Wellenius, G. A. (2020). Estimating the number of excess deaths attributable to heat in 297 United States counties. *Environmental Epidemiology*, *4*(3), e096. https://doi.org/10.1097/ee9.0000000000000096

White, R. H., Anderson, S., Booth, J. F., Braich, G., Draeger, C., Fei, C., et al. (2023). The unprecedented Pacific Northwest heatwave of June 2021. *Nature Communications*, *14*(1), 727. https://doi.org/10.1038/s41467-023-36289-3

Wick, G. A., Neiman, P. J., Ralph, F. M., & Hamill, T. M. (2013). Evaluation of forecasts of the water vapor signature of atmospheric rivers in operational numerical weather prediction models. *Weather and Forecasting*, *28*(6), 1337–1352. https://doi.org/10.1175/WAF-D-13-00025.1

World Meteorological Organization (WMO). (2021). State of the global climate WMO provisional report. Retrieved from https://library.wmo.int/doc_num.php?explnum_id=10859

Zhang, X., Zhou, T., Zhang, W., Ren, L., Jiang, J., Hu, S., et al. (2023). Increased impact of heat domes on 2021-like heat extremes in North America under global warming. *Nature Communications*, *14*(1), 1690. https://doi.org/10.1038/s41467-023-37309-y

Zuo, J., Pullen, S., Palmer, J., Bennetts, H., Chileshe, N., & Ma, T. (2015). Impacts of heat waves and corresponding measures: A review. *Journal of Cleaner Production*, *92*, 1–12. https://doi.org/10.1016/j.jclepro.2014.12.078